Supplemental Figure Legends

Supplemental Figure 1. TLR expression in pancreatic cancer. (A) Pancreata from 4 month old KPC (n=5) and PDX1-Cre;$Kras^{G12D}$; $Ink4a/Arf^{flox/flox}$ (n=2) mice were stained using an mAb directed against TLR7. Representative images are shown and the number of $TLR7^+$ cells per HPF was calculated. **(B)** A tissue microarray containing normal human pancreatic tissue (n=10), human pancreatic cancer (n=20), and tissue from patients with pre-invasive PanIN lesions (n=10) was stained for TLR7 and percentage of $TLR7^+$ cells as a fraction of all cells was determined for each group by examining 5 HPFs per tissue core. Representative images are shown**. (C)** TLR2 expression was tested in 6 month-old WT and p48Cre;$Kras^{G12D}$ mice using flow cytometry and gating on all $7AAD^-$ live cells. Data are representative of experiments performed twice using 2 mice per group. **(D)** Human pancreatic cancer specimens were tested for expression of TLR2 by IHC (n=5). A representative image is shown. Original magnifications, x40. Scale bars: 75μm.

Supplemental Figure 2. Pancreatic ductal epithelial cells exhibit the $CD45^-CD34^-CD133^+$ phenotype. (A) Pancreatic ductal epithelial cells were harvested from 6 months old p48Cre;$Kras^{G12D}$ mice as described (1, 2) and stained using mAbs directed against CD45, CD34, and CD133. Dashed histograms represent isotype controls. **(B)** Pancreatic $CD45^+$ inflammatory cells from 6 months old p48Cre;$Kras^{G12D}$ mice were gated and tested for expression of CD133 compared with isotype controls. Experiments were repeated twice with similar results.

Supplemental Figure 3. TLR7 ligation accelerates pancreatic carcinogenesis. (A, B) Six week old p48Cre;$Kras^{G12D}$ mice were administered saline or TLR7 ligand (ssRNA40) for 3 weeks or 6 weeks (n=4-5 mice per time point per group). **(A)** Representative image of pancreata at 3 weeks after treatment is shown. **(B)** Pancreas weights were recorded at the 3 and 6 week

time points. **(C)** Paraffin embedded pancreatic sections from p48Cre;Kras^{G12D} mice treated with ssRNA40 for 3 weeks beginning at 6 weeks of life were tested for the presence of invasive cancer (arrows) using an mAb directed against CK19. **(D)** Expression of TLR7 was measured in CD45^{+} and CD45^{-}CD34^{-}CD133^{+} cells from 9 week old WT or p48Cre**;**Kras^{G12D} mice that had been treated for 3 weeks with saline or ssRNA40 using 2 mice/group. **(E)** Six week old p48Cre;Kras^{G12D} mice were administered saline or TLR2 ligand (HKLM) for 3 weeks (n=3 mice per group). Representative H&E stained sections are shown. Original magnifications, x20. Scale bars: 150μm.

Supplemental Figure 4. ssRNA40 treatment results in loss of nuclear p16 in pancreatic ductal epithelial cells. Six week old p48Cre;Kras^{G12D} mice were administered saline or TLR7 ligand (ssRNA40) for 3 weeks. Confocal microscopy for p16/INK4A (red) was performed on frozen sections of pancreata from saline-treated (top panel) or TLR7 ligand-treated (bottom panel) p48Cre**;**Kras^{G12D} mice (n=3 mice/group). Actin fibers were stained with phalloidin (green); nuclei were counter-stained with DAPI (blue). Pancreatic ductal epithelial cells from ssRNA40-treated p48Cre**;**Kras^{G12D} mice exhibited loss of nuclear p16/INK4A in contrast to saline-treated mice. Representative images are shown. Original magnifications, x63.

Supplemental Figure 5. TLR7 inhibition alters expression of cell cycle regulatory genes in established tumors. 12 month old p48Cre;Kras^{G12D} mice were treated with saline or an oligonucliotide inhibitor of TLR7 (2 doses). Lysates were harvested from pancreata and expression of numerous cell cycle regulatory, pro-inflammatory, and oncogenic genes tested by Western blotting. Experiments were repeated twice with similar results using 2 mice per group.

Supplemental Figure 6. High pancreatic expression of TLR7 in benign fibro-inflammatory pancreatic disease. (A) Representative images of TLR7-stained paraffin-embedded pancreatic

sections from patients with chronic pancreatitis or **(B)** caerulein-treated mice with chronic pancreatitis (3 weeks of treatment). Original magnification, x40. Scale bar: 75μm. **(C)** The total number of $CD3^+CD4^+$ T cells, $CD3^+CD8^+$ T cells, $CD3^-CD19^+$ B cells, $CD11c^+MHCII^+$ dendritic cells, $Gr1^-CD11b^+$ macrophages, and $Gr1^+CD11b^+$ neutrophils staining positively for TLR7 per pancreas was calculated for both control pancreata and caerulein-induced acute pancreatitis using flow cytometry (n=5 mice per group; ***p<0.001). **(D)** Mice were treated with saline or caerulein for 48h in induce acute pancreatitis before sacrifice. Pancreatic single-cell suspensions were analyzed by flow cytometry. $CD45^+$ and $CD45^-$ cells were tested for expression of TLR7. The fraction of $CD45^+$ cells and TLR7 expressing subsets are shown. **(E)** Sub-gating on $CD34^-CD45^-CD133^+$ epithelial cells and $CD34^-CD45^-CD146^+$ endothelial cells revealed increased expression of TLR7 on ductal epithelial cells in acute pancreatitis. Median fluorescent indexes (MFI) are shown.

Supplemental Figure 7. TLR7 activation exacerbates pacreatitis in WT mice but does not alter expression cell cycle regulatory or oncogenic genes. (A) Paraffin embedded sections of pancreata from 9 week old WT mice that had been treated with for 3 weeks with caerulein or caerulein+ssRNA40 were stained for Insulin (Original magnification, x10. Scale bar: 300μm.), CD3, MPO (Original magnifications, x40. Scale bars: 75μm.), and B220 (Original magnification, x20. Scale bars: 150μm.). Representative images are shown. **(B)** Pancreatic islet cell area and **(C)** the extent of T cell, neutrophil, and B cell infiltrates were calculated (n=5/group; ***p<0.001). **(D)** Six week old WT and $TLR7^{-/-}$ mice were treated for two days with L-arginine to induce mild acute pancreatitis. Representative images are shown. Original magnification, x15. Scale bar: 225μm. n=3 mice/group. **(E)** Pancreatic lysates harvested from 9 week old from WT mice that had been treated for 3 weeks with saline, caerulein, ssRNA, or

caerulein + ssRNA were tested for expression of various cell cycle regulatory and oncogenic genes.

Supplemental Figure 8. Specificity of effects of TLR7 ligation in the pancreas. (A) Six week old WT mice were treated for three weeks with caerulein alone, caerulein + E. coli RNA, or caerulein + adenine analogue. Original magnification, x20. Scale bar: 150μm. n=3 mice/group. **(B)** To test the specificity of the effects of TLR7 agonists, WT and $TLR7^{-/-}$ mice were treated for three weeks with caerulein or caerulein+ssRNA40, respectively. Representative images of paraffin-embedded pancreatic sections are shown. Original magnification, x20. Scale bar: 150μm. n=3-4 mice/group. **(C)** To determine the effects of TLR7 ligation in absence of baseline pancreatic inflammation, WT mice were treated with saline, ssRNA40 alone, caerulein alone, or caerulein+ssRNA40. Representative H&E stained images are shown. Original magnification, x10. Scale bar: 300μm. n=4-6 mice/group.

Supplemental Figure 9. TLR7 ligation augments inflammation specifically within the pancreas (A) Representative H&E-stained sections of liver, kidney, lung, and small intestine from six week old WT mice treated with caerulein + ssRNA40. Original magnification, x20. Scale bar: 150μm. **(B)** Liver, kidney, lung, and small intestine were also stained for TLR7. Original magnification, x40. Scale bar: 75μm. n=3 mice/group.

Supplemental Figure 10. (A) CD45.1 mice were irradiated and made chimeric using bone marrow derived from CD45.2 mice. At 7 weeks splenocytes were harvested and the extent of chimerism determined by flow cytometry. **(B)** Two month-old WT mice were irradiated and made chimeric using either WT bone marrow (WT chimeric [WT]) or bone marrow derived from $TLR7^{-/-}$ mice ($TLR7^{-/-}$ chimeric [WT]). $TLR7^{-/-}$ mice were also made chimeric using WT bone marrow (WT chimeric [$TLR7^{-/-}$]). Seven weeks after chimerism, all three cohorts were subjected

to caerulein-induced acute pancreatitis for 4 consecutive days (n=3/group). Representative H&E (Original magnification, x20. Scale bar: 150μm) and CD45 (Original magnification, x40. Scale bar: 75μm) stained images are shown. Pancreatic edema and inflammatory cell infiltrate were quantified.

Supplemental Figure 11. TLR7-mediated pancreatic tumorigenesis interfaces with the Notch pathway and requires NF-κB and MAP Kinase signaling. (A-D) Lysates derived from whole pancreata from 9 week old WT or p48Cre;$Kras^{G12D}$ mice that had been treated for 3 weeks with saline or TLR7 ligand (ssRNA40) were equiloaded and tested by Western blotting using antibodies directed against **(A)** Notch1, **(B)** Notch 2, **(C)** Jagged1, Hes1, Hey1, **(D)** PPARγ, GAPDH, **(E)** IκBα, pIκBα, Erk1, pErk1, and β-actin. **(F)** Six week old p48Cre;$Kras^{G12D}$ mice were administered saline or TLR7 ligand (ssRNA40) for 3 weeks. Selected mice were simultaneously treated with the NEMO binding domain inhibitor or PD98059 to block NF-κB and MAP Kinase signaling, respectively. Representative H&E stained images are shown. Original magnification, x10. Scale bar: 300μm. n=4 mice/group.

Supplemental Figure 12. TLR7 agonists exacerbate pancreatic inflammation via NF-κB- and MAP kinase-dependent mechanisms. (A) Six week old WT mice were treated thrice weekly for four weeks with caerulein (C) to induce chronic pancreatitis. Selected mice were additionally treated with TLR7 ligand (ssRNA40). To determine the respective roles of NF-κB and MAP Kinase signaling, NF-$κB^{-/-}$ mice were treated, in parallel, with caerulein + ssRNA40 or WT mice were additionally treated with the MAP kinase inhibitor (PD98059). Original magnification, x10. Scale bar: 300μm. n=4-5 mice/group. **(B)** Pancreata from WT mice treated with caerulein or caerulein + ssRNA40 were tested for expression of NF-κB and MAP Kinase signaling intermediates by Western blotting.

References

1. Mallen-St Clair, J., Soydaner-Azeloglu, R., Lee, K.E., Taylor, L., Livanos, A., Pylayeva-Gupta, Y., Miller, G., Margueron, R., Reinberg, D., and Bar-Sagi, D. 2012. EZH2 couples pancreatic regeneration to neoplastic progression. *Genes & development* 26:439-444.

2. Agbunag, C., Lee, K.E., Buontempo, S., and Bar-Sagi, D. 2006. Pancreatic duct epithelial cell isolation and cultivation in two-dimensional and three-dimensional culture systems. *Methods in enzymology* 407:703-710.

Supplemental Figure 1

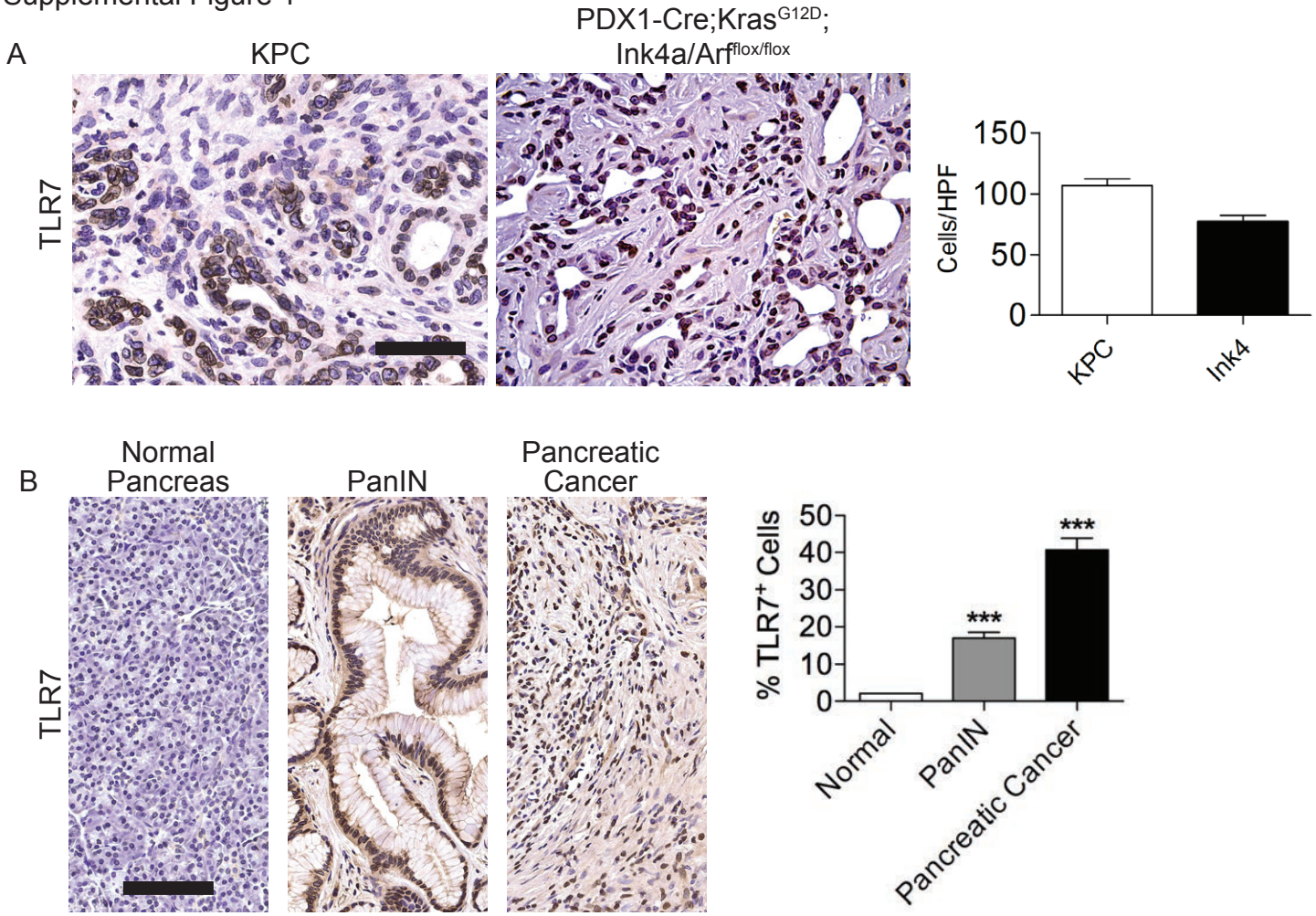

Supplemental Figure 2

A

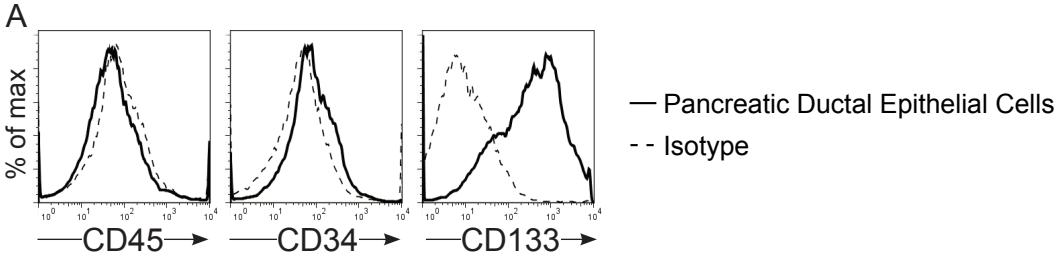

B

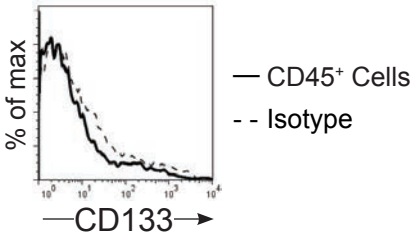

Supplemental Figure 3

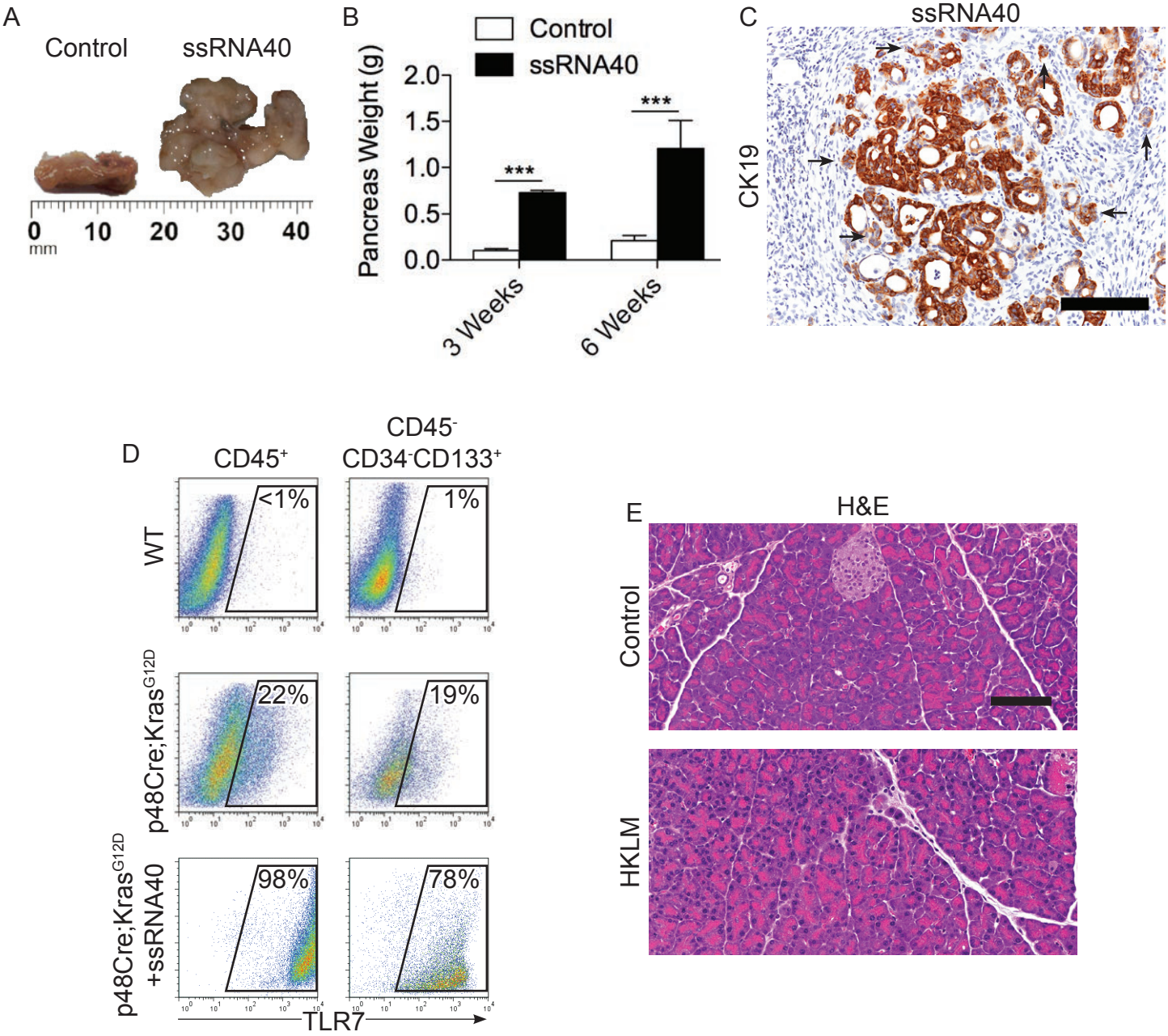

Supplemental Figure 4

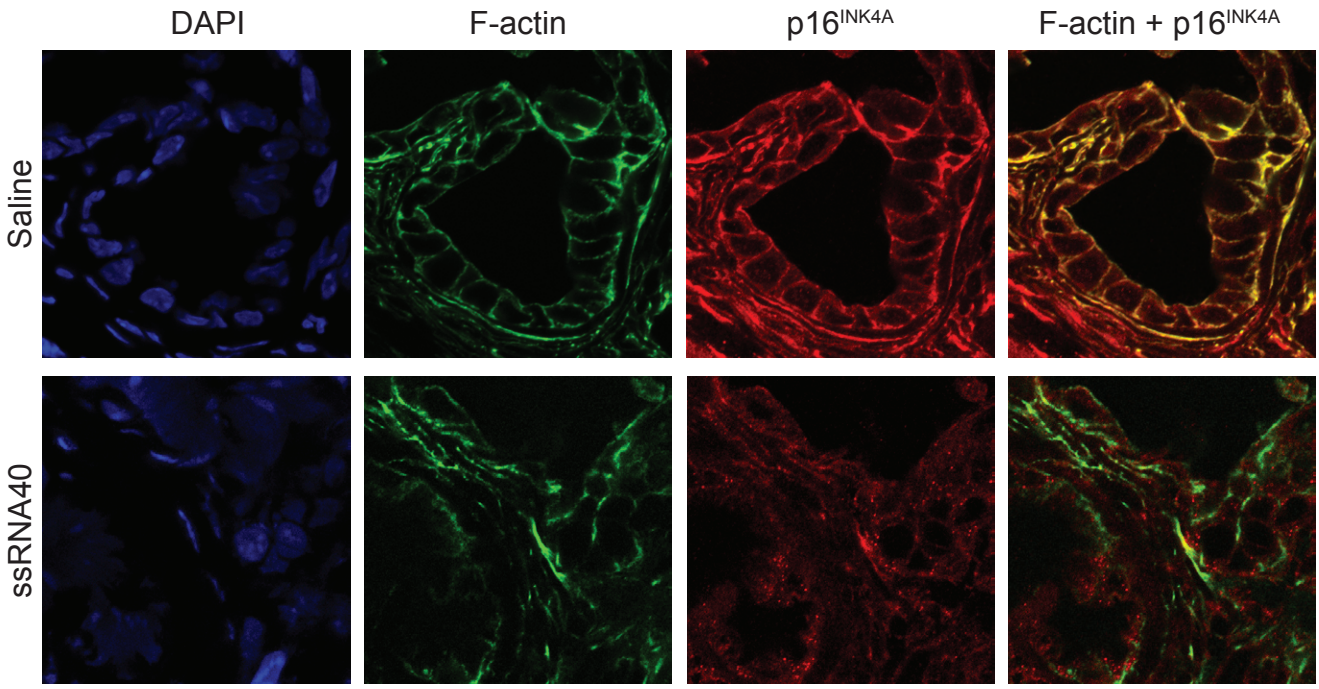

Supplemental Figure 5

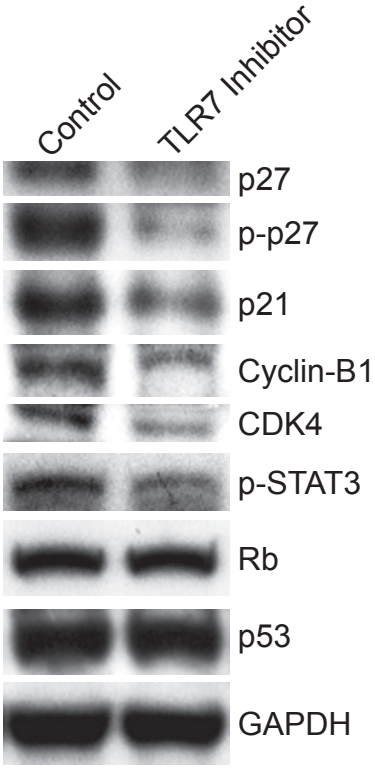

Supplemental Figure 6

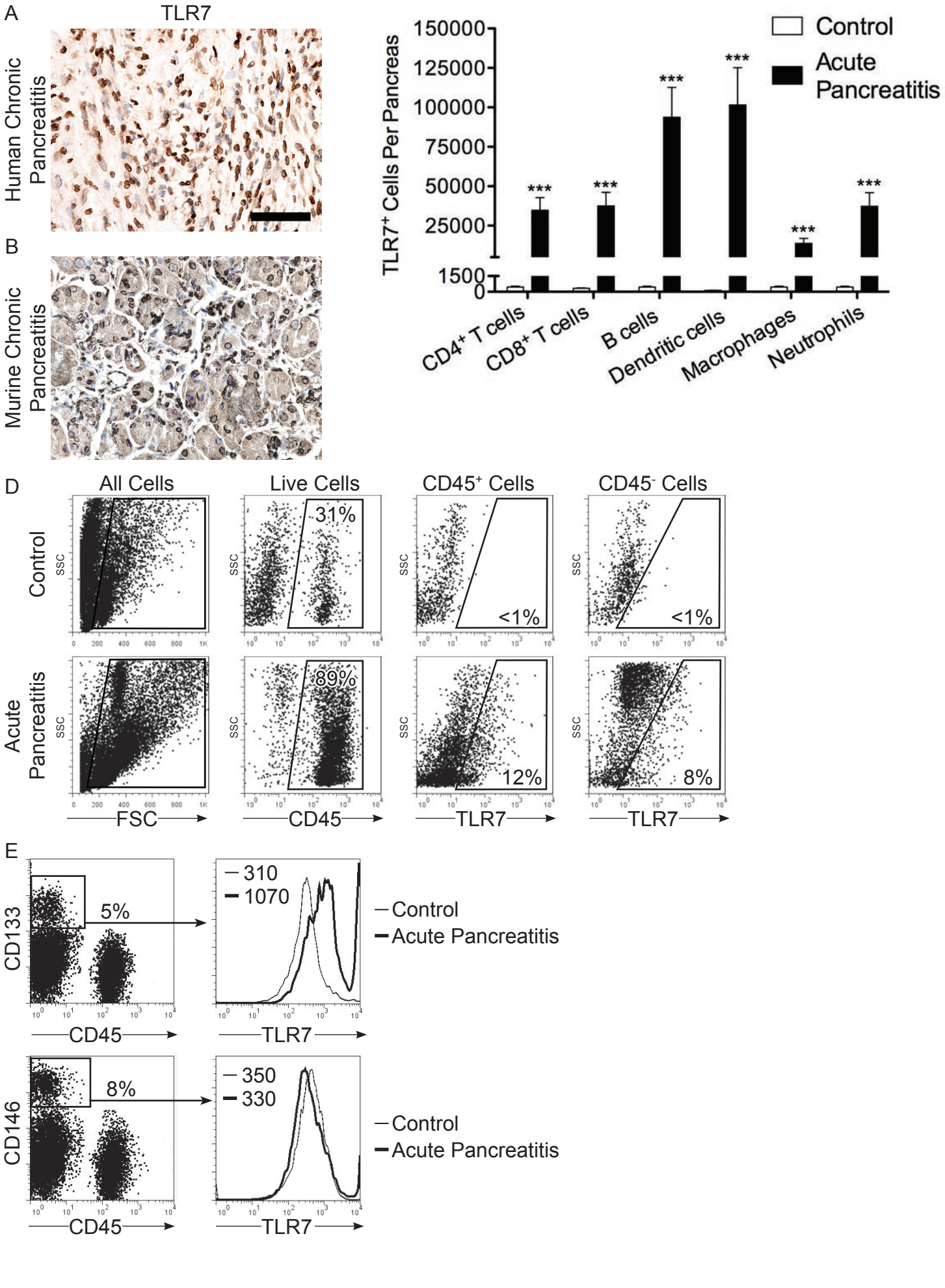

Supplemental Figure 7

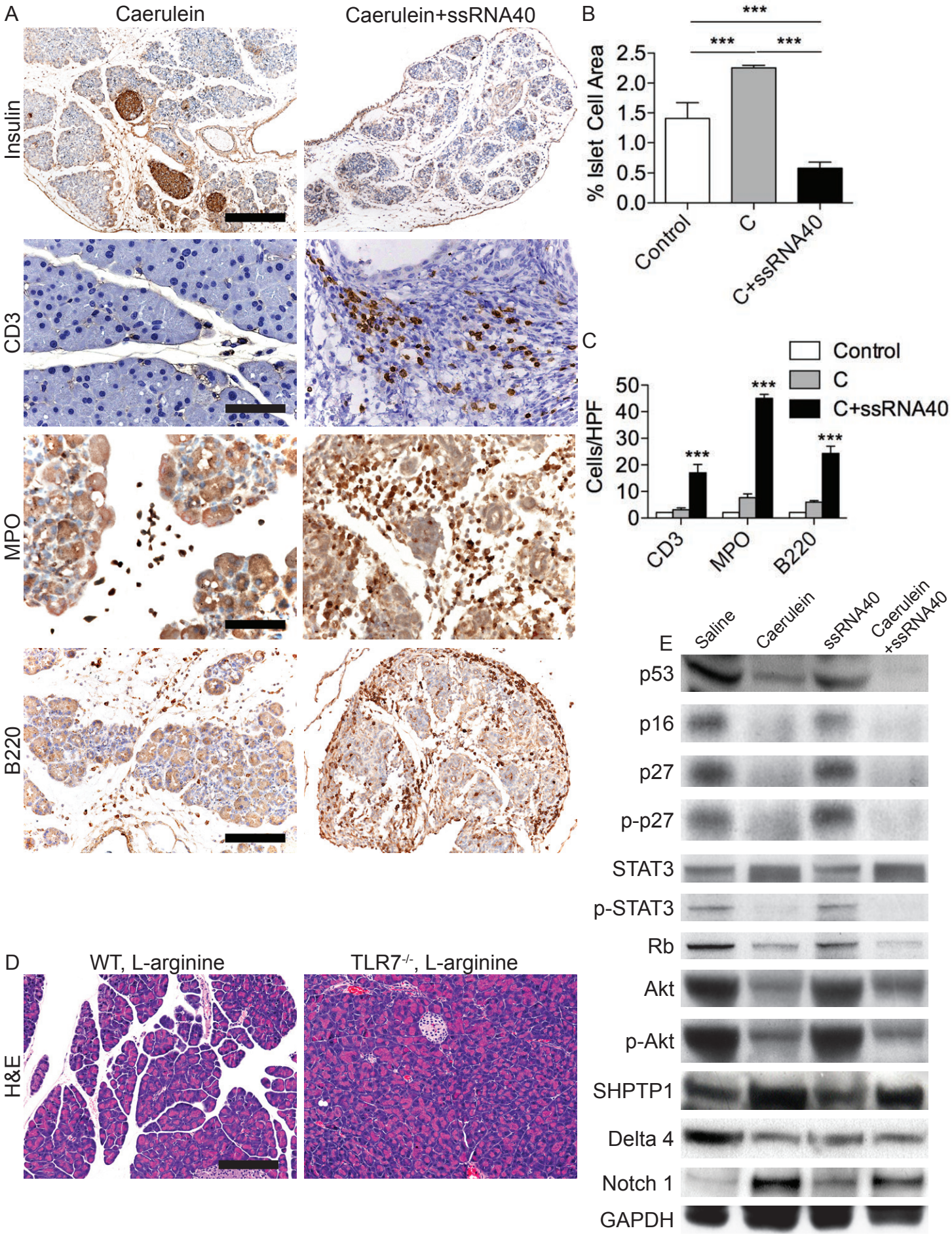

Supplemental Figure 8

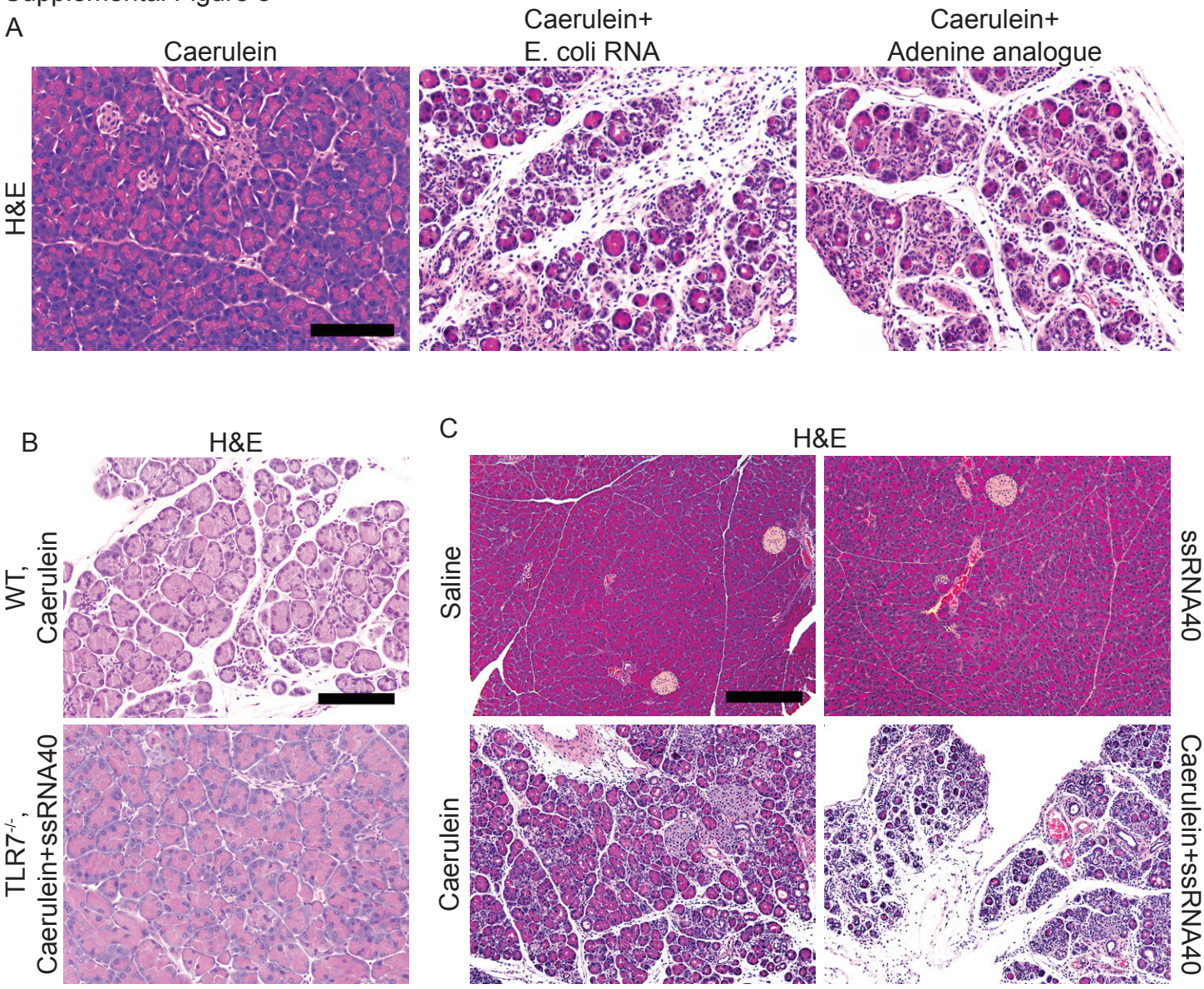

Supplemental Figure 9

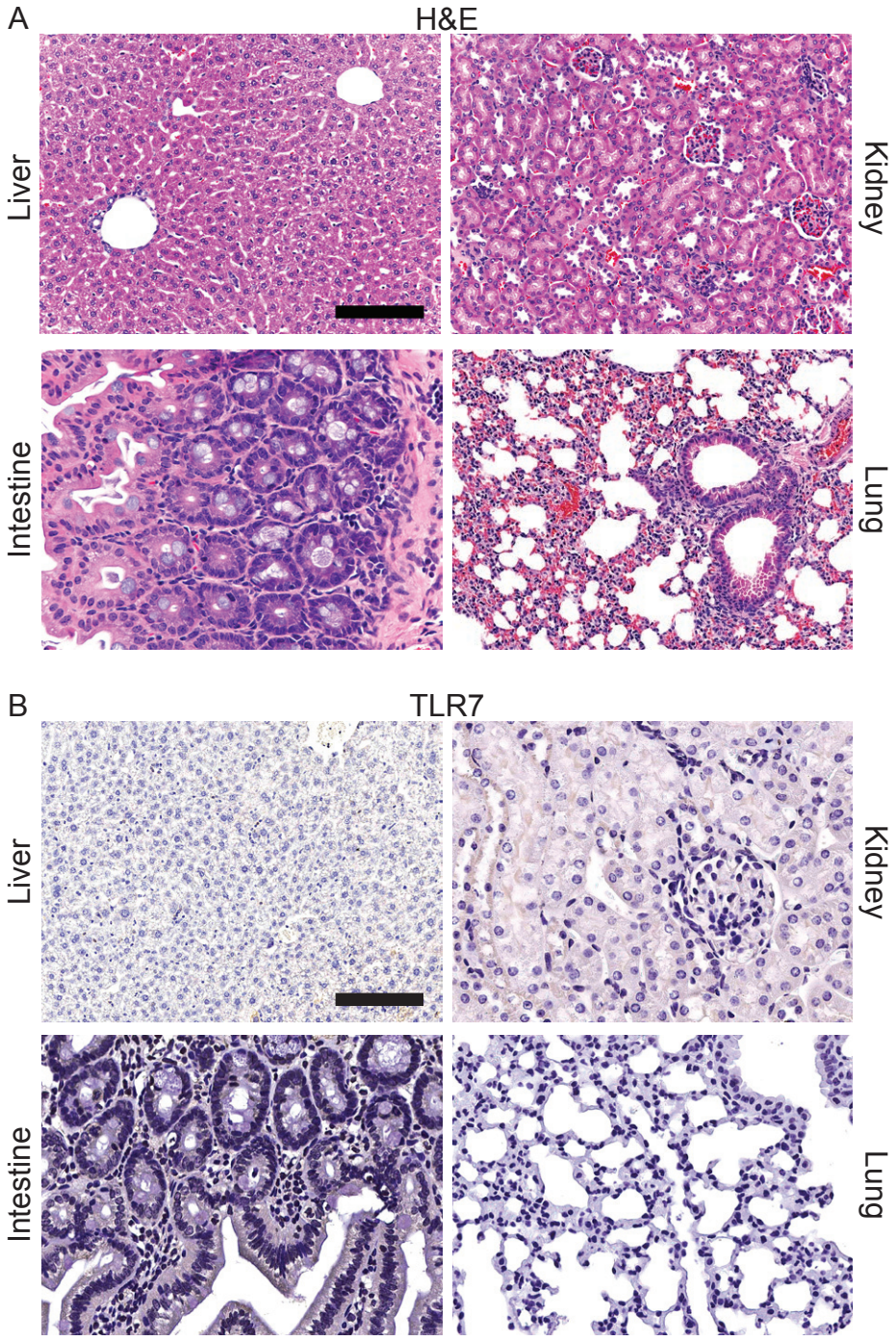

Supplemental Figure 10

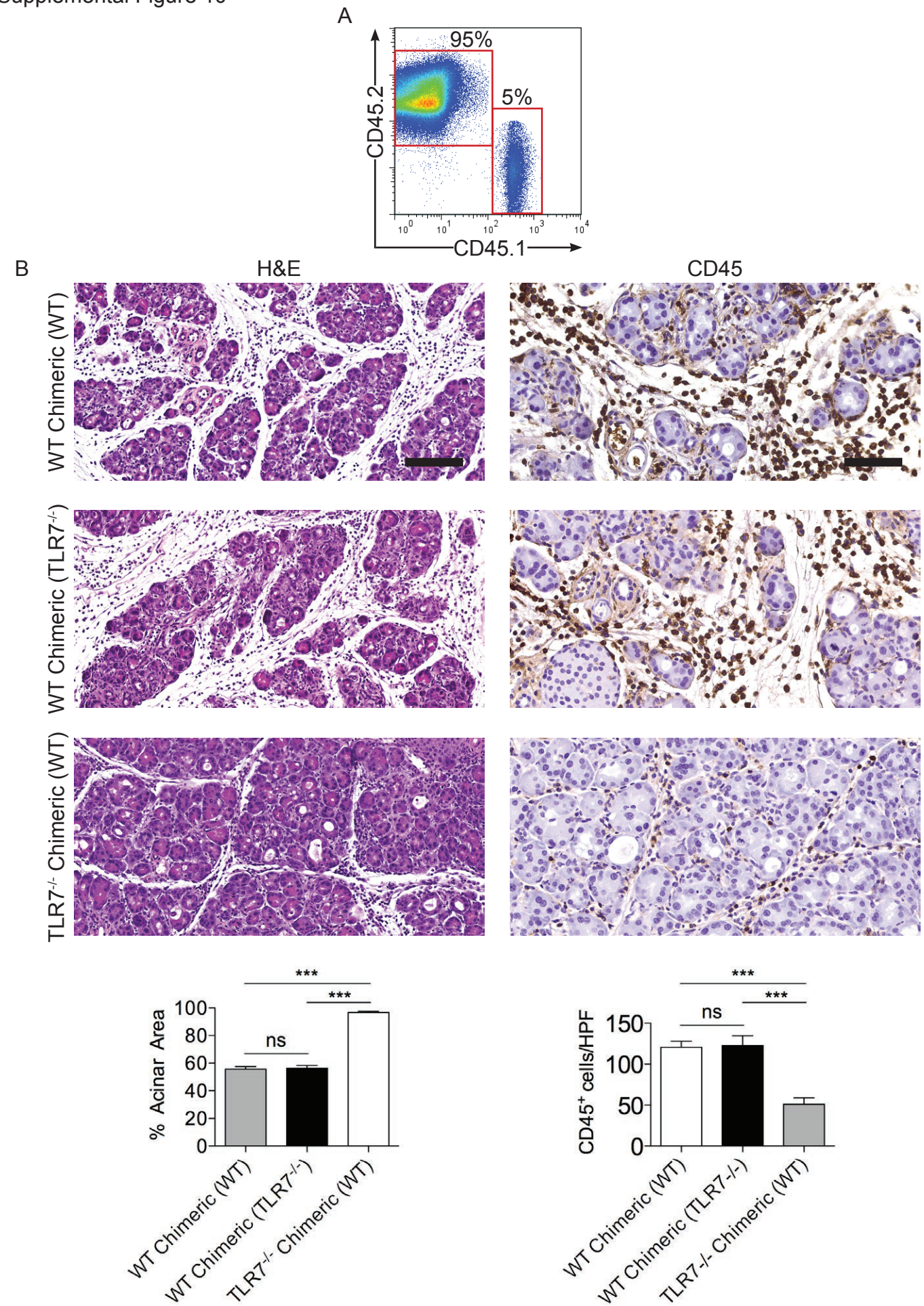

Supplemental Figure 11

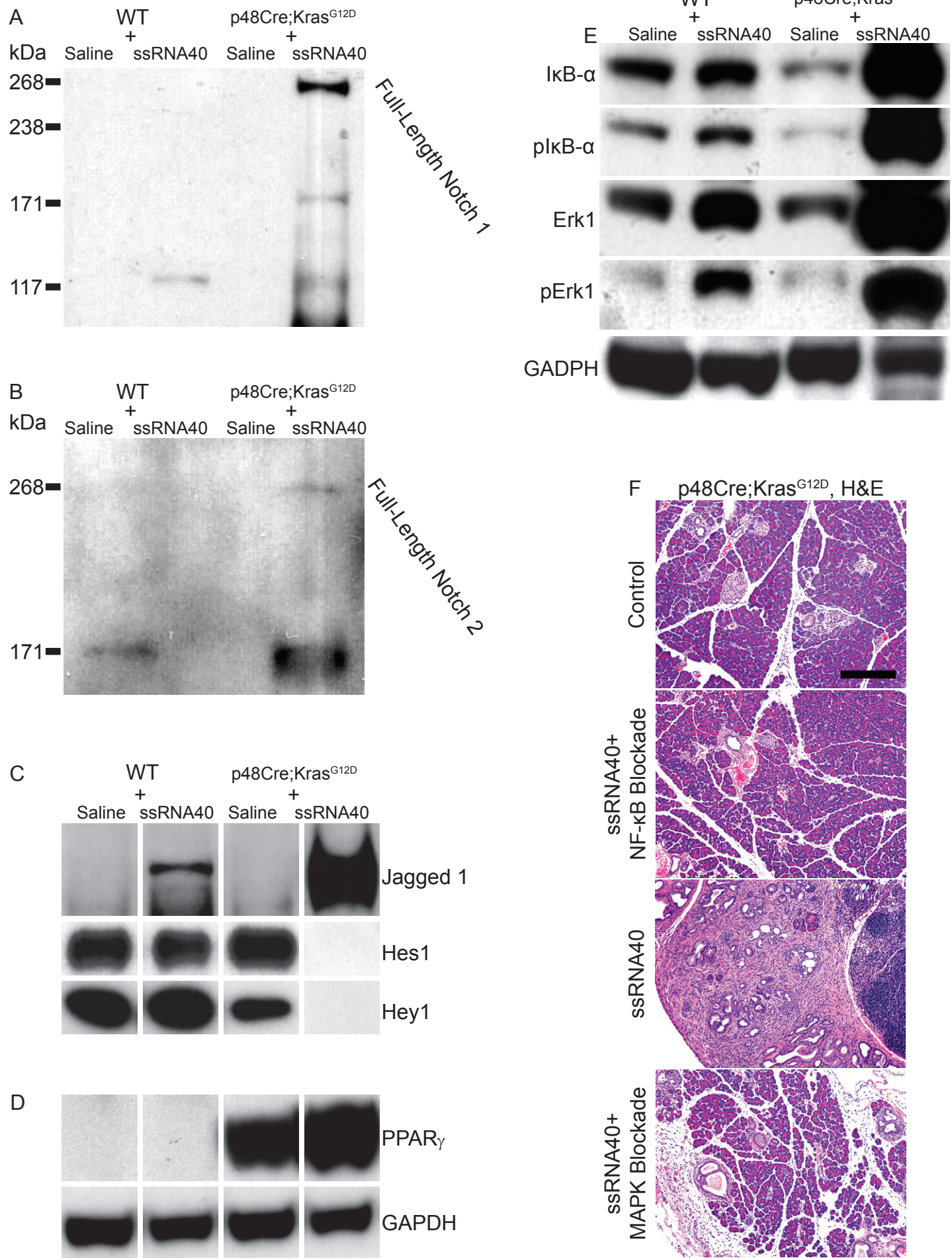

Supplemental Figure 12